ARTICLE

BIOTECHNOLOGY and BIOENGINEERING

Cellulose Solvent-Based Biomass Pretreatment Breaks Highly Ordered Hydrogen Bonds in Cellulose Fibers of Switchgrass

Noppadon Sathitsuksanoh,[1,2] Zhiguang Zhu,[1] Sungsool Wi,[3] Y.-H. Percival Zhang[1,2,4]

[1]Biological Systems Engineering Department, Virginia Polytechnic Institute and State University (Virginia Tech), 210-A Seitz Hall, Blacksburg, Virginia 24061; telephone: 540-231-7414, fax: 540-231-3199; e-mail: ypzhang@vt.edu

[2]Institute for Critical Technology and Applied Science (ICTAS), Virginia Polytechnic Institute and State University, Blacksburg, Virginia

[3]Chemistry Department, Virginia Polytechnic Institute and State University, Blacksburg, Virginia

[4]DOE BioEnergy Science Center (BESC), Oak Ridge, Tennessee

Received 25 June 2010; revision received 23 August 2010; accepted 4 October 2010

Published online 21 October 2010 in Wiley Online Library (wileyonlinelibrary.com). DOI 10.1002/bit.22964

ABSTRACT: The switchgrass (SG) samples pretreated by cellulose solvent- and organic solvent-based lignocellulose fractionation were characterized by enzymatic hydrolysis, substrate accessibility assay, scanning electron microscopy, X-ray diffraction (XRD), cross polarization/magic angle spinning (CP/MAS) ^{13}C nuclear magnetic resonance (NMR), and Fourier transform infrared spectroscopy (FTIR). Glucan digestibility of the pretreated SG was 89% at hour 36 at one filter paper unit of cellulase per gram of glucan. Crystallinity index (CrI) of pure cellulosic materials and SG before and after cellulose solvent-based pretreatment were determined by XRD and NMR. CrI values varied greatly depending on measurement techniques, calculation approaches, and sample drying conditions, suggesting that the effects of CrI data obtained from dried samples on enzymatic hydrolysis of hydrated cellulosic materials should be interpreted with caution. Fast hydrolysis rates and high glucan digestibilities for pretreated SG were mainly attributed to a 16.3-fold increase in cellulose accessibility to cellulase from 0.49 to 8.0 m^2/g biomass, because the highly ordered hydrogen-bonding networks in cellulose fibers of biomass were broken through cellulose dissolution in a cellulose solvent, as evidenced by CP/MAS ^{13}C-NMR and FTIR.

Biotechnol. Bioeng. 2011;108: 521–529.

KEYWORDS: biomass; biofuels; cellulose accessibility; cellulose solvent-based pretreatment; crystallinity index; drying of cellulose; switchgrass

Correspondence to: Y.-H. Percival Zhang

Contract grant sponsor: DOE BioEnergy Science Center (BESC)
Contract grant sponsor: USDA Biodesign and Bioprocessing Research Center (BBRC)
Contract grant sponsor: ICTAS Scholar Program

Introduction

The production of biofuels and biobased products from renewable cellulosic biomass would promote rural economy, decrease greenhouse gas emissions, and enhance national energy security (Lynd et al., 2002; Zhang, 2009). The current production of second generation biofuels, cellulosic ethanol, cannot compete with that made from corn and sugarcane, because of high processing costs, the requirement for huge capital investment, and relatively low revenues from low-value ethanol (Zhang, 2008). Biomass saccharification usually involves two sequential steps: lignocellulose pretreatment/fractionation and enzymatic hydrolysis. The root causes of biomass recalcitrance have been attributed to several factors: low substrate accessibility to enzymes, high crystallinity of cellulose, presence of hemicellulose, lignin, and other components, and high degree polymerization of cellulose chains (Zhang and Lynd, 2004; Himmel et al., 2007; Rollin et al., 2010). Highly ordered hydrogen bonds and *van der Waals* forces among sugar chains in crystalline fibers result in high crystallinity index (CrI) values and very low substrate accessibility (Lynd et al., 2002; Hong et al., 2007).

Switchgrass (SG) (*Panicum virgatum* L.) is a native, warm-seasoned, perennial, C_4 grass in North America and is distributed in more than half of the United States. It has several valuable features, such as modest/high productivities, adaptation to many types of soil and climate,

efficient water use, and low input of fertilizers and herbicides (i.e., high ratio of energy output to energy input). Therefore, SG has been regarded as a promising bioenergy crop.

Cellulose solvent- and organic solvent-based lignocellulose fractionation (COSLIF) has been developed to fractionate lignocellulose by using a combination of a concentrated phosphoric acid as a cellulose solvent and an organic solvent (e.g., acetone or ethanol) under modest reaction conditions (Zhang et al., 2007; Sathitsuksanoh et al., 2009). Concentrated phosphoric acid beyond a critical concentration disrupts the linkage among cellulose, hemicellulose, and lignin through biomass dissolution and increases cellulose accessibility greatly (Moxley et al., 2008). Our earlier work has shown that COSLIF-pretreated biomass can be hydrolyzed quickly by cellulase with very high glucan digestibilities (Zhang et al., 2007; Sathitsuksanoh et al., 2009; Zhu et al., 2009).

Crystallinity index (CrI) of cellulose is widely regarded as a key substrate characteristic that affects enzymatic cellulose hydrolysis (Chang and Holtzapple, 2000; Laureano-Perez et al., 2005), because amorphous cellulose can be hydrolyzed much faster than crystalline cellulose (Zhang et al., 2006). Some studies showed that crystallinity of cellulosic materials increased over the course of enzymatic cellulose hydrolysis (Betrabet and Paralikar, 1977; Ooshima et al., 1983), while others represent contradictory results (Ohmine et al., 1983; Puls and Wood, 1991). Many techniques, such as X-ray diffraction (XRD) (Teeäär et al., 1987), cross polarization/magic angle spinning (CP/MAS) ^{13}C nuclear magnetic resonance (CP/MAS ^{13}C-NMR) (Newman, 1999; Park et al., 2009), and Fourier-transform infrared spectroscopy (FTIR) (Oh et al., 2005) have been employed to determine CrI values. Park et al. (2009) have presented significantly different crystallinity values for the same materials by XRD and CP/MAS ^{13}C-NMR approaches (Park et al., 2009). Therefore, CrI roles in biomass pretreatment and enzymatic hydrolysis remain in debate.

Drying conditions of cellulosic samples greatly influence their characteristics and rates of enzymatic hydrolysis (Fan et al., 1980; Laivins and Scallan, 1996; Zhang and Lynd, 2004). Saddler and co-workers (Esteghlalian et al., 2001) show that different drying methods greatly affect substrate accessibility measured by Simon's stain. Oven drying results in the collapse or closure of the large pores in the samples, accompanied with significant reductions in enzymatic hydrolysis rates. Therefore, it is recommended to measure cellulose accessibility to cellulase (CAC) under hydrated conditions without drying (Hong et al., 2007).

In this study, we applied COSLIF pretreatment to SG. In order to understand the extent of CrI on enzymatic hydrolysis, many characteristics of SG and pure cellulosic materials before and after the pretreatment were investigated via scanning electron microscopy (SEM), XRD, CP/MAS ^{13}C-NMR, and FTIR. Moreover, effects of drying conditions (i.e., air drying and freeze drying) on enzymatic hydrolysis and substrate characteristics were studied.

Materials and Methods

Chemicals and Materials

All chemicals were reagent grade and purchased from Sigma–Aldrich (St. Louis, MO), unless otherwise noted. Phosphoric acid (85%) and ethanol (95%) were purchased from Fisher Scientific (Houston, TX). The *Trichoderma* cellulase (Novozyme® 50013) and β-glucosidase (Novozyme® 50010) were donated by Novozymes North America (Franklinton, NC). They had activities of 84 filter paper units (FPU)/mL and 270 cellobiase units/mL, respectively. Microcrystalline cellulose (Avicel PH105) was purchased from FMC (Philadelphia, PA). Regenerated amorphous cellulose (RAC) was prepared through Avicel dissolution in concentrated phosphoric acid, followed by regeneration in water as described elsewhere (Zhang et al., 2006). Birchwood xylan was purchased from Sigma–Aldrich. Lignin was isolated from sugar cane bagasse through Kraft pulping and NaOH treatment at 170°C. SG was procured from the National Renewable Energy Laboratory (Boulder, CO). The naturally dried SG was milled into small particles by a Pallmann counter-rotating knife ring flaker (Clifton, NJ). The resulting particulates were screened to the nominal sizes of 40-60 mesh. Bovine serum albumin was purchased from Alfa Aesar (Ward Hill, MA).

COSLIF Procedure

The COSLIF pretreatment was conducted as described elsewhere (Zhang et al., 2007), with some modifications. The COSLIF was conducted using 85% H_3PO_4 at 50°C, 1 atm, and 45 min. Acetone was replaced with 95% (v/v) ethanol (Sathitsuksanoh et al., 2009; Sathitsuksanoh et al., 2010). The residual amorphous solid pellets were neutralized to pH 5–7 with a small amount of 2 M sodium carbonate. The air-drying COSLIF-pretreated switchgrass (PSG) samples were prepared by direct drying in a Precision oven (Thermo Fisher Scientific Inc., Waltham, MA) at 37°C for 24 h. The freeze-drying samples were frozen at −70°C for 60 min and then was lyophilized in a VirTis freeze-drying apparatus (Gardiner, NY).

Carbohydrate and Lignin Assays

The structural carbohydrate composition of SG was determined by a modified quantitative saccharification (QS) procedure (Moxley and Zhang, 2007). In the modified QS, the secondary hydrolysis was conducted in the presence of 1% (w/w) sulfuric acid, rather than 4% (w/w) sulfuric acid at 121°C, for 1 h, creating a more accurate determination of acid-labile carbohydrates (e.g., xylan and arabinan). Monomeric sugars were measured by a Shimadzu HPLC equipped with a Bio-Rad Aminex HPX-87P column (Richmond, CA). Lignin and ash were measured according to the standard NREL biomass protocol (Sluiter et al., 2006; Moxley and Zhang, 2007). The concentrations of glucose

and xylose in the enzymatic hydrolysate were measured by a Shimadzu HPLC (Columbia, MD) with a Bio-Rad Aminex HPX-87H chromatography column equipped with refractive index detector. Galactose and mannose were co-eluted with xylose. The column was operated with 5 mM H_2SO_4 as a mobile phase at 60°C and at a flow rate of 0.6 mL/min.

Enzymatic Hydrolysis

The COSLIF-PSG samples were diluted to 10 g glucan/L in a 50 mM sodium citrate buffer (pH 4.8) with supplementary addition of 0.1% (w/v) NaN_3. All hydrolysis experiments were carried out in a rotary shaker at 250 rpm and 50°C. Four enzyme loadings were tested: 15, 10, 5, and 1 FPU of cellulase, supplemented with 10 units of β-glucosidase per gram of glucan. After enzymatic hydrolysis, enzymatic hydrolysis digestibility for glucan was calculated as previously described (Zhang et al., 2009).

Crystallinity Index Assays and Calculations

The CrI value can be determined by XRD and CP/MAS ^{13}C-NMR, along with different calculation approaches. The X-ray diffractograms of all samples were measured by the PANalytical X'Pert Pro X-ray diffractometer (Westborough, MA) with CoKα radiation ($\lambda = 1.78901$ Å) with the scanning rate of 4°/min ranging from 10° to 60°. With and without amorphous halo correction, deconvolution of the XRD spectra was conducted using PeakFit® 4.12 software (Systat Software Inc., Chicago, IL) assuming Gaussian distribution function as the shape of the resolved peaks. With regard to the peak height method, the CrI value was calculated based on the height of the peak corresponding to (002) lattice plane (I_{002}) and the minimum between 110 and 002 lattice planes (I_{am}) as below (Segal et al., 1959; Zhang and Lynd, 2004).

$$CrI\ (\%) = \frac{I_{002} - I_{am}}{I_{002}} \times 100$$

Based on the peak-deconvolution method, five crystalline peaks corresponding to (101), (10$\bar{1}$), (021), (002), and (040) lattice planes. These crystalline scattering is superimposed on an amorphous scattering. The spectra were deconvolved using Gaussian line shape function. The CrI value was calculated from the ratio of the crystalline area over the total area (Park et al., 2009). Based on the amorphous subtraction method, the separation of peaks from amorphous and crystalline contributions were conducted by subtracting the scattering of an amorphous standard (Ruland, 1961), where xylan was chosen as an amorphous standard. The CrI value was calculated from the ratio of the crystalline area over the total area after all spectra were deconvolved by using Gaussian line shape function.

The cross-polarization magic-angle spinning (CP/MAS) ^{13}C-NMR spectra of all samples were obtained on a Bruker II Avance-300 spectrometer operating at the resonance frequencies of 300.12 MHz for 1H, and 75.47 MHz for ^{13}C, using a Bruker 4.0 mm MAS NMR probe spinning at 6 kHz. Cross-polarization for 1 ms mixing time was achieved at 50 kHz rf-field at the 1H channel and linearly ramping the ^{13}C rf-field over a 25% range centered at 38 kHz. Total accumulation time was 8 min (2048 transient signals) by using 63 kHz of two-pulse phase modulated proton decoupling technique (Bennett et al., 1995). All spectra were collected at room temperature with polyethylene as an internal standard. According to the C_4 peak-deconvolution method, the CrI value was calculated from the ratio of the crystalline area over the total area, where separation of crystalline (86–92 ppm) and amorphous (79–86 ppm) fractions were based on Guassian line shape function. According to the NMR amorphous subtraction method, amorphous contribution was separated from the original spectrum prior to deconvolution of signals in the C_4 resonance region, where xylan was an amorphous standard.

Other Assays

The total substrate accessibility to cellulase (TSAC), CAC, and non-cellulose accessibility to cellulase (NCAC) were determined based on the maximum adsorption capacity of the TGC protein containing a green fluorescence protein and a cellulose-binding module (Zhu et al., 2009; Rollin et al., 2010). The recombinant TGC fusion protein was produced in *Escherichia coli* BL21 (pNT02) (Hong et al., 2007) and purified by affinity adsorption (Hong et al., 2008). The SEM images of the biomass materials were taken with a Zeiss-DSM940 (Carl Zeiss, Okerkochen, Germany), as described elsewhere (Moxley et al., 2008). All samples were sputter-coated with gold and imaged by SEM. All FTIR spectra were subjected to Saviszky-Golay smoothing. The absorbance of the bands obtained were resolved using Voigt distribution function by PeakFit® 4.12 software. The FTIR spectroscopy was conducted using a Thermo Nicolet 6700 ATR/FT-IR spectrometer (Thermo Fisher Scientific Inc.). Two hundred and fifty-six scans at a resolution of 6/cm were averaged for each sample.

Results

Enzymatic Hydrolysis of COSLIF-Pretreated Switchgrass

Switchgrass samples were pretreated by the modified COSLIF procedure, where ethanol was used as an organic solvent (Sathitsuksanoh et al., 2009). The completely dry SG contained 34.6% glucan, 18.6% xylan, 1.9% galactan, 3.0% arabinan, 21.0% lignin, as well as 20.9% extractives, ashes, and proteins. After COSLIF pretreatment, PSG contained 43.4% glucan, 8.2% xylan, 1.0% galactan, 1.0% arabinan, and 20.3% lignin.

The glucan hydrolysis profiles of the COSLIF-PSG were examined at different enzyme loadings from 1 to

15 FPU/g of glucan (Fig. 1). At a high enzyme loading of 15 FPU/g of glucan (~9.9 mg cellulase/g of glucan), glucan digestibility reached 94.6% at hour 24. When cellulase loading was reduced, glucan digestibility decreased slightly. At a low cellulase loading of 1 FPU/g of glucan (~0.67 mg cellulase/g of glucan), glucan digestibilities were 68% at hour 12, 83% at hour 24, and 92% at hour 72.

At hour 12, low cellulase loadings resulted in low glucan digestibilities. However, the glucan digestibility still reached 92% at hour 72 when enzyme loading was only 1 FPU of cellulase/g of glucan. A 15-fold reduction in cellulase loading for hydrolysis while maintaining high glucan digestibility would greatly reduce the amount of costly cellulase required for soluble sugar release.

Supramolecular Structure and Substrate Accessibility

The drastic changes in the surface morphology of SG before and after COSLIF were observed by using SEM (Fig. 2). The intact SG shows fiber cells (Fig. 2A). By contrast, PSG had no obvious fibrous structure (Fig. 2B and C), suggesting that all fibrous structures of the lignocellulose were completely disrupted by cellulose solvent-based pretreatment.

Substrate accessibilities of SG were measured based on adsorption of a non-hydrolytic fusion protein TGC (Zhu et al., 2009). Through COSLIF pretreatment, TSAC and CAC increased from 1.3 ± 0.1 to $9.6 \pm 0.6\ m^2/g$ of biomass and from 0.49 ± 0.05 to $8.0 \pm 1.1\ m^2/g$, respectively (Table I). A drastic increase in CAC by 16.3-fold led to high enzymatic digestibilities and fast hydrolysis rates even at low enzyme loadings. The two-fold increase in NCAC, from 0.78 to 1.62 m^2/g of biomass, was lower than the 16.3-fold increase in CAC, suggesting the accessibility of the cellulose fraction is preferably increased by COSLIF, compared to other cellulase-adsorptive surfaces in the pretreated biomass.

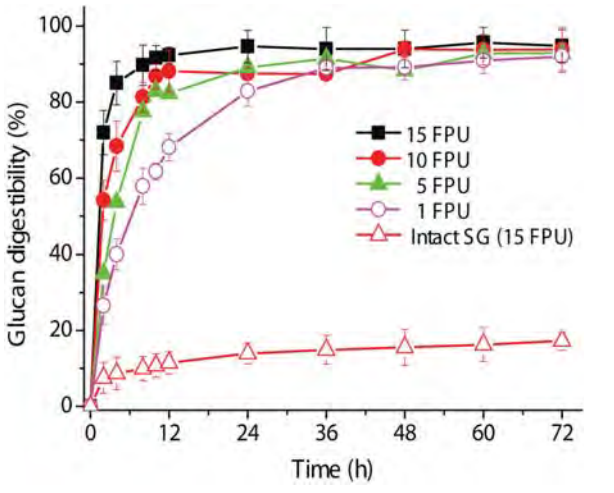

Figure 1. Enzymatic cellulose hydrolysis profiles for the COSLIF-PSG at different enzyme loading: 1, 5, 10, and 15 FPU of cellulase, supplemented by 10 units of β-glucosidase per gram of glucan. [Color figure can be seen in the online version of this article, available at wileyonlinelibrary.com.]

X-Ray Diffraction Analysis

The XRD spectra of Avicel, RAC, xylan, and lignin are shown in Figure 3A. The XRD spectrum of Avicel showed five peaks, corresponding to (101), (10$\bar{1}$), (021), (002), and (040) lattice planes of crystalline cellulose I polymorph. The XRD spectrum of freeze-dried RAC, which was made from dissolution of Avicel and precipitation in water, showed a significant reduction in intensities of these five peaks. The intensities of peaks corresponding to (101), (10$\bar{1}$), and (040) lattice planes were greatly reduced to an undetectable level. The remaining two peaks corresponding to (021) and (002) lattice planes were broader and weaker than those of Avicel, indicating a significant reduction in crystallinity after cellulose dissolution and regeneration. A similar spectrum was observed for the air-dried RAC. However, the intensities of peaks of air-dried RAC corresponding to (021) and (002) lattice planes were higher than those of freeze-dried RAC, implying an increase in crystallinity due to air drying. Xylan and lignin did not exhibit any significant peaks, indicating that they are amorphous (Fig. 3A).

The XRD spectra of intact SG, air-dried PSG, and freeze-dried PSG are shown in Figure 3B. The spectrum of intact SG showed two significant peaks corresponding to (101) and (002) lattice planes. The peaks corresponding to (10$\bar{1}$), (021), and (040) lattice planes were not observed, which might be due to interference from other components in SG (e.g., hemicellulose and lignin), which may affect the peak broadening while part of a composite with cellulose. The spectrum of freeze-dried PSG showed a drastic reduction of intensity of the 101 peak to an undetectable level. The 002 peak in freeze-dried PSG was greatly reduced compared to that of intact SG, indicating a significant reduction in crystalline fraction of SG via COSLIF. Similar to the spectrum of freeze-dried PSG, the spectrum of air-dried PSG showed a broad 002 peak. Comparison of intensities of the peaks between freeze- and air-dried PSG spectra showed slightly different spectra; based on CrI calculation method, different conclusions may be drawn about the relative crystallinity of these different drying conditions.

Effect of Drying on Enzymatic Cellulose Hydrolysis

Previous work suggested that drying might greatly change the characteristics of hydrated cellulosic materials (Fan et al., 1981; Weimer et al., 1990; Zhang and Lynd, 2004). Since enzymatic cellulose hydrolysis must be conducted in hydrated conditions, we investigated the effects of air drying and freeze drying on enzymatic hydrolysis of PSG (Fig. 4A) and pure cellulose (Fig. 4B). The wet PSG was hydrolyzed fast at an enzyme loading of 15 FPU/g of glucan, reaching more than 90% digestibility within 12 h (Fig. 4A).

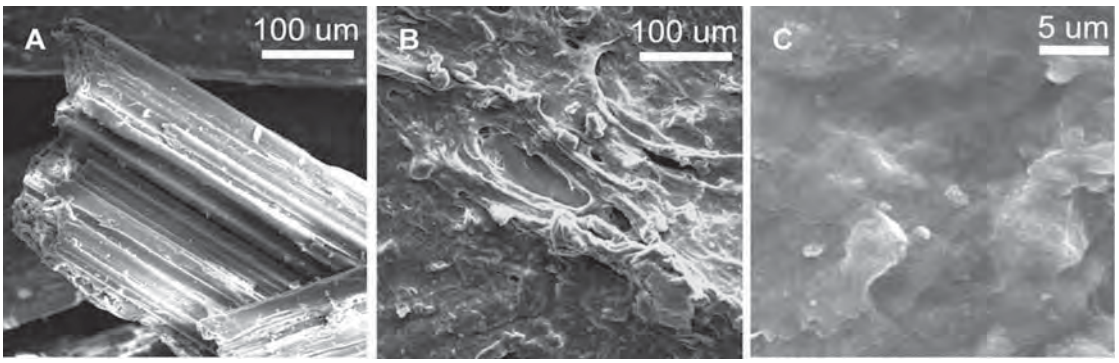

Figure 2. SEM micrographs of SG samples before (**A**) and after the COSLIF pretreatment (**B** and **C**).

Air-dried PSG that was hydrated before enzymatic hydrolysis had a poor digestibility of 63% at hour 72, suggesting that air drying caused a great reduction in substrate reactivity possibly due to a collapse in its supramolecular structures. The freeze-dried sample had a similar hydrolysis profile to hydrated COSLIF-PSG, suggesting that freeze drying can better preserve the substrate structure and reactivity compared to air drying, but still decrease the substrate accessibility relative to samples that were never dried (Table I). For both PSG (Fig. 4A) and pretreated pure cellulose (Fig. 4B), air drying resulted in a great reduction of enzymatic substrate reactivity which cannot be recovered by re-hydration, while freeze drying largely preserved the substrate reactivity.

Solid State ^{13}C-NMR Spectroscopy

Solid-state ^{13}C-NMR spectrum of Avicel (Fig. 5A) exhibited six singlets corresponding to ^{13}C chemical shifts of cellulose carbons, C_1 (105 ppm), C_4 (79–92 ppm), $C_2/C_3/C_5$ (70–80 ppm), and C_6 (60–69 ppm) of the anhydroglucose units of cellulose (Dudley et al., 1983). The C_4 resonance region is commonly used for determining cellulose crystallinity (Isogai et al., 1989). Moreover, the changes in the C_6 resonance region may indicate changes of specific hydrogen bonding with other hydroxyl groups in the adjacent cellulose chains. Broad shoulders in the C_4 region at 83 ppm and in the C_6 region at 63 ppm indicate the presence of amorphous cellulose (Atalla et al., 1980). Our NMR spectrum of Avicel showed strong signals at 89 and 65 ppm and broad signals at 83 and 63 ppm, indicating that Avicel contains both crystalline and amorphous fractions. In comparison with Avicel, the NMR spectrum of freeze-dried RAC showed a reduction in signals at 89 and 65 ppm, suggesting a decrease in crystalline fractions and possible disruption of orderly hydrogen-bonding networks in cellulose dissolution and regeneration. Similar results were observed in the air-dried pretreated sample.

Table I. Total substrate accessibility to cellulase (TSAC), cellulose accessibility to cellulase (CAC), and non-cellulose accessibility to cellulase (NCAC).

Materials	TSAC (m^2/g biomass)	CAC (m^2/g biomass)	NCAC (m^2/g biomass)
Intact switchgrass	1.3 ± 0.1	0.49 ± 0.05	0.78 ± 0.09
COSLIF-pretreated switchgrass[a]	9.6 ± 0.6	8.0 ± 1.1	1.6 ± 1.3
Freeze-dried COSLIF-pretreated switchgrass	2.7 ± 0.4	2.1 ± 0.4	0.59 ± 0.40
Avicel		2.3 ± 0.1	
RAC[a]		51.9 ± 0.9	
Freeze-dried RAC		19.1 ± 1.3	

[a]Never-dried samples.

The CP/MAS ^{13}C-NMR spectra of intact SG, air-dried PSG, and freeze-dried PSG are shown in Figure 5B. The spectrum of intact SG showed a broad C_4 region (79–92 ppm) and a peak at 65 ppm with a shoulder (63 ppm) in the C_6 region. PSG regardless of drying means did not show significant differences in the C_4 region. The broader C_4 regions for SG samples (Fig. 5B) than that of Avicel (Fig. 5A) may be attributed to the presence of hemicellulose and lignin in SG. After COSLIF pretreatment, the peak in the C_6 region (65 ppm) appeared to be weaker relative to that of intact SG, indicating that highly ordered hydrogen-bonding networks in SG was disrupted by using COSLIF.

The spectrum of isolated lignin (Fig. 5A) shows a strong signal at 56 ppm, corresponding to aromatic methoxyl (–OCH_3) resonance (Bartuska et al., 1980; Maciel et al., 1981). The NMR spectrum of intact SG exhibits a weak peak signal at 56 ppm, indicating a presence of lignin (Fig. 5B). After COSLIF pretreatment, air-dried PSG shows a very weak peak at 56 ppm while there is no significant peak at 56 ppm in freeze-dried PSG sample, implying that lignin characteristics may be changed by different drying methods.

Fourier Transform Infrared Spectroscopy Analysis

Comparison of FTIR spectra of Avicel and RAC shows differences in band intensities at 898 (ν_{as}(ring), anomeric

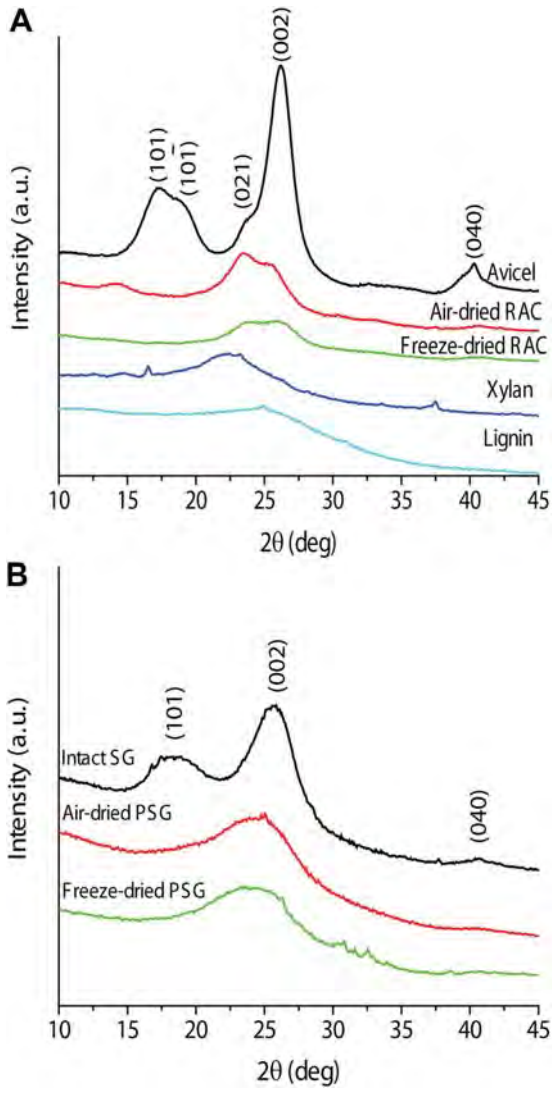

Figure 3. XRD spectra of Avicel, air-dried RAC, freeze-dried RAC, xylan, and lignin (**A**), as well as intact SG, PSG samples followed by air drying or freeze drying, and wet PSG that was never dried (**B**). [Color figure can be seen in the online version of this article, available at wileyonlinelibrary.com.]

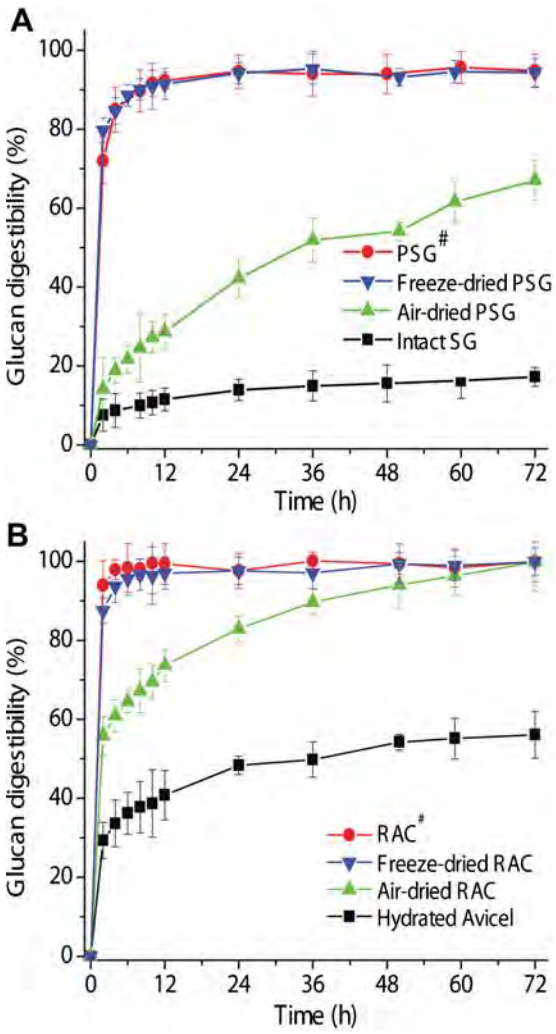

Figure 4. Enzymatic cellulose hydrolysis profiles of intact SG, air-dried PSG, and freeze-dried PSG (**A**), and Avicel, RAC, air-dried RAC, and freeze-dried RAC (**B**). #Never-dried samples. [Color figure can be seen in the online version of this article, available at wileyonlinelibrary.com.]

vibration at β-glycosidic linkage), 1055 (ν(CO), CO stretching), 1105 (ν_{as}(ring), antisymmetric in-phase ring stretching), 1161 (ν_{as}(COC), COC antisymmetric stretching), 1281 (δ(CH), CH bending), 1315 (ω(CH_2), CH_2 wagging), 1335 (δ(OH), OH rocking), 1368 (δ(CH), CH bending), 1428 (δ_s(CH_2), CH_2 symmetric bending), and 2897 (ν(CH), CH stretching) cm^{-1} whose assignments are given in parentheses (Nelson and O'Connor, 1964; Hulleman et al., 1994; Dumitriu, 1998). Figure 6A shows that these band intensities decrease from Avicel to RAC, implying that highly ordered hydrogen bonds in Avicel were disrupted through cellulose dissolution and regeneration. The air-dried RAC showed stronger band intensities at 2897 and 898 cm^{-1} than freeze-dried RAC, suggesting that some RAC may re-crystallize during air drying, as partially supported by an increase in the peak intensity corresponding to the (002) lattice plane in the XRD spectra (Fig. 3A).

The FTIR spectra of intact SG and freeze-dried PSG are shown in Figure 6B. The freeze-dried PSG sample showed more significant decreases in the band intensities at 2919, 1422, 1368, 1337, 1319, 1158, and 898 cm^{-1} than intact SG, suggesting that highly ordered hydrogen bonds in crystalline cellulose of SG were disrupted after the pretreatment.

Discussion

Crystallinty is believed to be a key substrate characteristic affecting enzymatic hydrolysis. However, these results presented here suggest that the different conclusion can be drawn. Table II shows the CrI values of pure cellulosic materials and pretreated biomass by XRD employing three

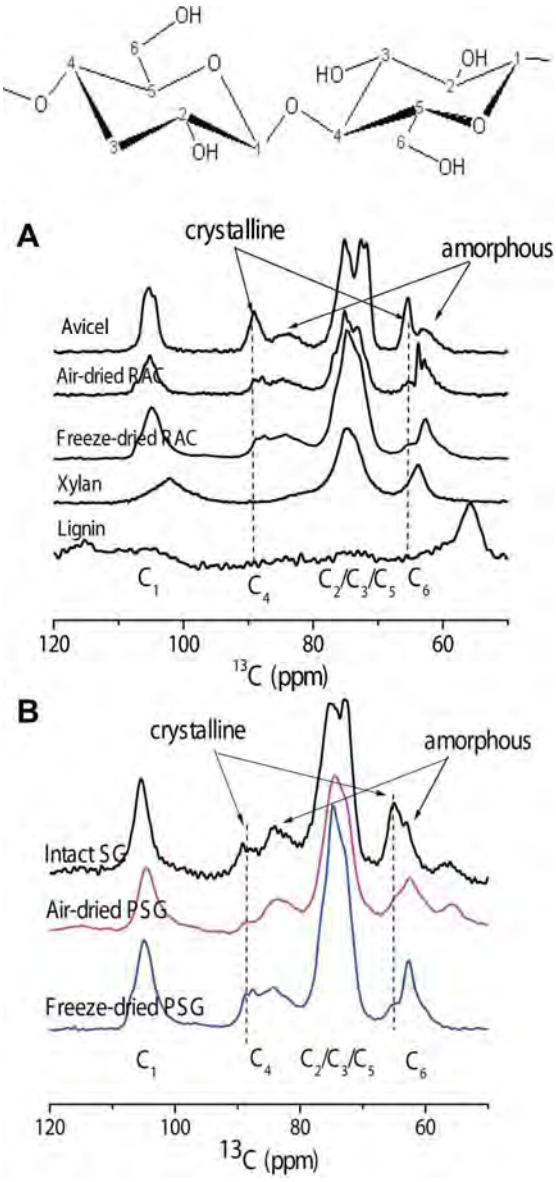

Figure 5. CP/MAS ^{13}C-NMR spectra of intact SG, air-dried PSG, and freeze-dried PSG. [Color figure can be seen in the online version of this article, available at wileyonlinelibrary.com.]

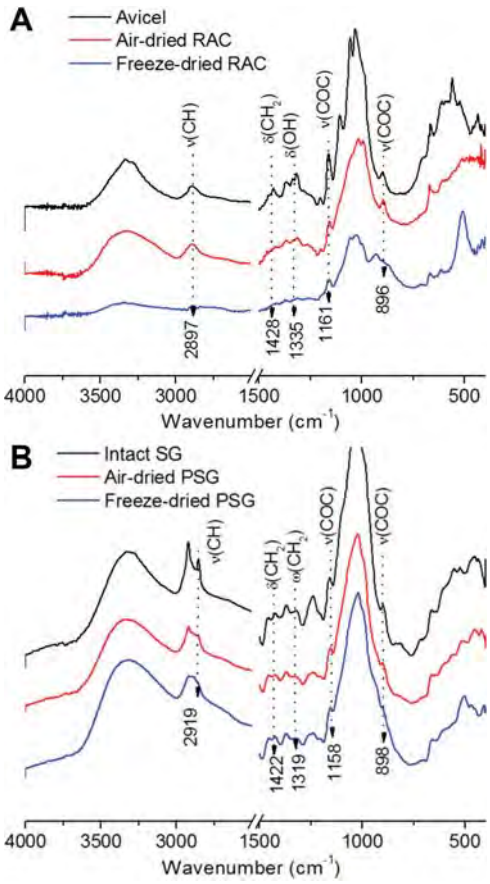

Figure 6. FTIR spectra of Avicel, air-dried RAC, and freeze-dried RAC (**A**), as well as intact SG, air-dried PSG, and freeze-dried PSG (**B**). [Color figure can be seen in the online version of this article, available at wileyonlinelibrary.com.]

different calculation approaches based on peak height (Segal et al., 1959; Zhang and Lynd, 2004), peak deconvolution (Teeäär et al., 1987), and amorphous subtraction (Ruland, 1961), as well as CP/MAS ^{13}C-NMR using two different calculation approaches based on C_4 peak separation (Newman, 1999), and NMR amorphous subtraction (Park et al., 2009). CrI values of Avicel ranged from 52.8% to 91.8%, depending on the measurement techniques and calculation approaches. CrI values of Avicel from NMR were ~53–58%, suggesting that Avicel is a mixture of crystalline and amorphous cellulose, while the CrI value from the peak height method via XRD was 91.8%, suggesting that Avicel was highly crystalline. CrI values were 70.0% and 73.1% for Avicel based on peak-deconvolution and amorphous substration via XRD, respectively. These large variations in dry Avicel suggested that CrI determination were influenced greatly by the techniques and calculation means. RAC samples have no detectable CrI values (Table II). Amorphous subtraction-based NMR methods showed that air-dried RAC had a much higher CrI value than freeze-dried RAC, indicating that air drying may re-crystallize some fractions of amorphous cellulose.

Measurement of the CrI value of lignocellulose is more complicated than that of pure cellulose because the presence of hemicellulose, lignin and other components interferes with the fingerprint regions of cellulose. The CrI values of intact SG ranged from 33.6% to 67.0%, depending on its measurement techniques and calculation methods (Table II). After pretreatment, freeze-dried PSG had much lower CrI values (between 3.2% and 32.0%). Clearly, COSLIF greatly reduced crytallinity of biomass.

The relationship among CrI changes, pretreatment efficacies and subsequent enzymatic hydrolysis is very complicated. Some biomass pretreatments, such as COSLIF and ionic liquid-based pretreatment, decrease CrI values

Table II. The CrI values of pure and pretreated cellulosic materials by different measurement techniques and calculation approaches.

Materials	CrI (%)				
	XRD			NMR	
	Peak height	Peak de-convolution	Amorphous subtraction[a]	C_4 peak separation	Amorphous subtraction[a]
Dry Avicel	91.8	70.0	73.1	53.2	58.2
Air-dried RAC	ND	ND	ND	ND	33.5
Freeze-dried RAC	ND	ND	ND	ND	5.7
Intact switchgrass	67.0	59.4	60.9	38.9	33.6
Air-dried COSLIF-pretreated switchgrass	12.5	10.9	ND	21.8	15.6
Freeze-dried COSLIF-pretreated switchgrass	3.2	14.0	ND	17.6	19.1

ND, not detectable.
[a]Xylan was chosen as a standard for amorphous subtraction calculations via XRD and CP/MAS ^{13}C-NMR.

greatly by disrupting highly ordered hydrogen bonds in crystalline cellulose fibers (Gollapalli et al., 2002; Lee et al., 2009; Zhao et al., 2009). By contrast, other biomass pretreatments, such as dilute acid and steam explosion, increased composite CrI values by removing amorphous fractions (i.e., hemicellulose) (Deschamps et al., 1996; Kim and Lee, 2005). Considering the multiple facts that: (i) the CrI values of lignocellulose are mainly correlated with crystalline cellulose fraction, (ii) the composite CrI values of lignocellulose are also influenced by other lignocellulose components, such as hemicellulose and lignin, (iii) CrI determination is greatly influenced by measurement techniques, calculation methodologies, and drying conditions during sample preparation (Table II), and (iv) enzymatic hydrolysis is heavily influenced by substrate characteristics (e.g., cellulose accessibility), remaining hemicellulose and lignin, as well as properties of remaining lignin. We believe that the determination of CrI values of biomass after pretreatment lose some significance relating to glucan digestibility and pretreatment efficacy.

Conclusions

COSLIF-PSG was hydrolyzed fast with high digestibility at low enzyme loadings because the cellulose solvent (concentrated phosphoric acid) disrupted the linkage among cellulose, hemicelluloses, and lignin, as well as dissolved cellulose fibers, resulting in disruption of highly ordered hydrogen bonds in crystalline cellulose in SG, as evidenced by CP/MAS ^{13}C-NMR and FTIR. The CrI values for the pure cellulosic materials and SG varied largely, depending on its measurement techniques, calculation means, and drying conditions for the sample preparation. These results suggested that CrI was not a key substrate characteristic impacting enzymatic cellulose hydrolysis and relating to pretreatment efficacy.

This work was supported partially by the DOE BioEnergy Science Center (BESC), USDA Bioprocessing and Biodesign Center, and DuPont Young Professor Award. NS was partially supported by the ICTAS Scholar Program. The BioEnergy Science Center is a U.S. Department of Energy Bioenergy Research Center supported by the Office of Biological and Environmental Research in the DOE Office of Science. The authors were grateful to Drs. Justin Barone and William Reynolds of Virginia Polytechnic and State University for their assistance in FTIR and XRD analysis. We would like to express our gratitude to Dr. Scott Renneckar for providing the isolated lignin utilized in this study, as well as Dr. Hugo Azurmendi for access and assistance to the NMR facility. We also would like to thank Dr. Sunkyu Park of North Carolina State University for his helpful discussions on CrI determination.

References

Atalla R, Gast J, Sindorf D, Bartuska V, Maciel G. 1980. 13C NMR spectra of cellulose polymorphs. J Am Chem Soc 102(9):3249–3251.

Bartuska V, Maciel G, Bolker H, Fleming B. 1980. Structural studies of lignin isolation procedures by 13C NMR. Holzforschung 34(6):214–217.

Bennett A, Rienstra C, Auger M, Lakshmi K, Griffin R. 1995. Heteronuclear decoupling in rotating solids. J Chem Phys 103:6951–6958.

Betrabet SM, Paralikar KM. 1977. Effect of cellulase on the morphology and fine structure of cellulosic substrates: Part 1. wheat straw pulp. Cell Chem Technol 11:615–625.

Chang VS, Holtzapple MT. 2000. Fundamental factors affecting biomass enzymatic reactivity. Appl Biochem Biotechnol 84-6: 5–37.

Deschamps FC, Ramos LP, Fontana JD. 1996. Pretreatment of sugar cane bagasse for enhanced ruminal digestion. Appl Biochem Biotechnol 57-58:171–182.

Dudley R, Fyfe C, Stephenson P, Deslandes Y, Hamer G, Marchessault R. 1983. High-resolution carbon-13 CP/MAS NMR spectra of solid cellulose oligomers and the structure of cellulose II. J Am Chem Soc 105(8):2469–2472.

Dumitriu S (editor). 1998. Polysaccharides: Structural diversity and functional versatility. New York, NY: CRC Press, p.1147.

Esteghlalian A, Bilodeau M, Mansfield S, Saddler J. 2001. Do enzymatic hydrolyzability and Simons' stain reflect the changes in the accessibility of lignocellulosic substrates to cellulase enzymes? Biotechnol Prog 17(6):1049–1054.

Fan LT, Lee Y-H, Beardmore DH. 1980. Mechanism of the enzymatic hydrolysis of cellulose: Effects of major structural features of cellulose on enzymatic hydrolysis. Biotechnol Bioeng 22:177–199.

Fan LT, Lee Y-H, Beardmore DR. 1981. The influence of major structural features of cellulose on rate of enzymatic hydrolysis. Biotechnol Bioeng 23:419–424.

Gollapalli LE, Dale BE, Rivers DM. 2002. Predicting digestibility of ammonia fiber explosion (AFEX)-treated rice straw. Appl Biochem Biotechnol 98/100:23–35.

Himmel ME, Ding S-Y, Johnson DK, Adney WS, Nimlos MR, Brady JW, Foust TD. 2007. Biomass recalcitrance: Engineering plants and enzymes for biofuels production. Science 315(5813):804–807.

Hong J, Ye X, Zhang Y. 2007. Quantitative determination of cellulose accessibility to cellulase based on adsorption of a nonhydrolytic fusion protein containing CBM and GFP with its applications. Langmuir 23(25):12535–12540.

Hong J, Ye X, Wang Y, Zhang Y-HP. 2008. Bioseparation of recombinant cellulose binding module-protein by affinity adsorption on an ultra-high-capacity cellulosic adsorbent. Anal Chem Acta 621:193–199.

Hulleman S, Vanhazendonk J, Vandam J. 1994. Determination of crystallinity in native cellulose from higher-plants with diffuse-reflectance Fourier-transform infrared-spectroscopy. Carbohyd Res 261:163–172.

Isogai A, Usuda M, Kato T, Uryu T, Atalla R. 1989. Solid-state CP/MAS carbon-13 NMR study of cellulose polymorphs. Macromolecules 22(7): 3168–3172.

Kim TH, Lee. YY. 2005. Pretreatment and fractionation of corn stover by ammonia recycle percolation process. Biores Technol 96:2007–2013.

Laivins G, Scallan A. 1996. The influence of drying and beating on the swelling of fines. J Pulp Paper Sci 22(5):J178–J184.

Laureano-Perez L, Teymouri F, Alizadeh H, Dale. B. 2005. Understanding factors that limit enzymatic hydrolysis of biomass. Appl Biochem Biotechnol 124(1):1081–1099.

Lee SH, Doherty TV, Linhardt RJ, Dordick JS. 2009. Ionic liquid-mediated selective extraction of lignin from wood leading to enhanced enzymatic cellulose hydrolysis. Biotechnol Bioeng 102(5):1368–1376.

Lynd LR, Weimer PJ, van Zyl WH, Pretorius IS. 2002. Microbial cellulose utilization: Fundamentals and biotechnology. Microbiol Mol Biol Rev 66:506–577.

Maciel G, O'Donnell D, Ackerman J, Hawkins B, Bartuska V. 1981. A 13C NMR study of four lignins in the solid and solution states. Die Makromol Chem 182(8):2297–2304.

Moxley G, Zhang Y-HP. 2007. More accurate determination of acid-labile carbohydrate composition in lignocellulose by modified quantitative saccharification. Energy Fuels 21:3684–3688.

Moxley GM, Zhu Z, Zhang Y-HP. 2008. Efficient sugar release by the cellulose solvent based lignocellulose fractionation technology and enzymatic cellulose hydrolysis J. Agric Food Chem 56(17):7885–7890.

Nelson M, O'Connor R. 1964. Relation of certain infrared bands to cellulose crystallinity and crystal latticed type. Part I. Spectra of lattice types I, II, III and of amorphous cellulose. J Appl Polym Sci 8(3):1311–1324.

Newman R. 1999. Estimation of the lateral dimensions of cellulose crystallites using 13C NMR signal strengths. Solid State Nucl Magn Reson 15(1):21–29.

Oh S, Yoo D, Shin Y, Seo G. 2005. FTIR analysis of cellulose treated with sodium hydroxide and carbon dioxide. Carbohydr Res 340(3):417–428.

Ohmine K, Ooshima H, Harano Y. 1983. Kinetic study of enzymatic hydrolysis of cellulose by cellulase from *Trichoderma viride*. Biotechnol Bioeng 25:2041–2053.

Ooshima H, Sakata M, Harano Y. 1983. Adsorption of cellulase from *Trichoderma viride* on cellulose. Biotechnol Bioeng 25:3103–3114.

Park S, Johnson D, Ishizawa C, Parilla P, Davis M. 2009. Measuring the crystallinity index of cellulose by solid state 13C nuclear magnetic resonance. Cellulose 16(4):641–647.

Puls J, Wood. TM. 1991. The degradation pattern of cellulose by extracellular cellulases of aerobic and anaerobic microorganisms. Biores Technol 36:15–19.

Rollin JA, Zhu Z, Sathisuksanoh N, Zhang Y-HP. 2010. Increasing substrate accessibility is more important than removing lignin: A comparison of cellulose solvent-based lignocellulose fractionation and soaking in aqueous ammonia. Biotechnol Bioeng DOI: 10.1002/bit.22919.

Ruland W. 1961. X-ray determination of crystallinity and diffuse disorder scattering. Acta Crystallogr 14:1180–1184.

Sathitsuksanoh N, Zhu Z, Templeton N, Rollin J, Harvey S, Zhang Y-HP. 2009. Saccharification of a potential bioenergy crop, *Phragmites australis* (common reed), by lignocellulose fractionation followed by enzymatic hydrolysis at decreased cellulase loadings. Ind Eng Chem Res 48:6441–6447.

Sathitsuksanoh N, Zhu Z, Ho T-J, Bai M-D, Zhang Y-HP. 2010. Bamboo saccharification through cellulose solvent-based biomass pretreatment followed by enzymatic hydrolysis at ultra-low cellulase loadings. Biores Technol 101:4926–4929.

Segal L, Creely J, Martin A, Jr., Conrad C. 1959. An empirical method for estimating the degree of crystallinity of native cellulose using the X-ray diffractometer. Text Res J 29(10):786.

Sluiter A, Hames B, Ruiz R, Scarlata C, Sluiter J, Templeton D, Crocker D. 2008. Determination of structural carbohydrates and lignin in biomass. National Renewable Energy Laboratory, Golden, CO, USA. NREL Laboratory Analytical Procedure.

Teeäär R, Serimaa R, Paakkarl T. 1987. Crystallinity of cellulose, as determined by CP/MAS NMR and XRD methods. Polym Bull 17(3): 231–237.

Weimer PJ, Lopez-Guisa JM, French AD. 1990. Effect of cellulose fine structure on kinetics of its digestion by mixed ruminal microorganisms *in vitro*. Appl Environ Microbiol 56:2421–2429.

Zhang Y-HP. 2008. Reviving the carbohydrate economy via multi-product biorefineries. J Ind Microbiol Biotechnol 35(5):367–375.

Zhang Y-HP. 2009. A sweet out-of-the-box solution to the hydrogen economy: Is the sugar-powered car science fiction? Energy Environ Sci 2(2):272–282.

Zhang Y-HP, Lynd LR. 2004. Toward an aggregated understanding of enzymatic hydrolysis of cellulose: Noncomplexed cellulase systems. Biotechnol Bioeng 88:797–824.

Zhang Y-HP, Cui J-B, Lynd LR, Kuang LR. 2006. A transition from cellulose swelling to cellulose dissolution by o-phosphoric acid: Evidences from enzymatic hydrolysis and supramolecular structure. Biomacromolecules 7(2):644–648.

Zhang Y-HP, Ding S-Y, Mielenz JR, Elander R, Laser M, Himmel M, McMillan JD, Lynd. LR. 2007. Fractionating recalcitrant lignocellulose at modest reaction conditions. Biotechnol Bioeng 97(2):214–223.

Zhang Y-HP, Berson E, Sarkanen S, Dale BE. 2009. Pretreatment and biomass recalcitrance: fundamentals and progress. Appl Biochem Biotechnol 153:80–83.

Zhao H, Jones CL, Baker GA, Xia S, Olubajo O, Person VN. 2009. Regenerating cellulose from ionic liquids for an accelerated enzymatic hydrolysis. J Biotechnol 139(1):47–54.

Zhu Z, Sathitsuksanoh N, Vinzant T, Schell DJ, McMillan JD, Zhang Y-HP. 2009. Comparative study of corn stover pretreated by dilute acid and cellulose solvent-based lignocellulose fractionation: Enzymatic hydrolysis, supramolecular structure, and substrate accessibility. Biotechnol Bioeng 103:715–724.